Title: Gray matter vulnerabilities predict longitudinal development of apathy in Huntington's disease.

Audrey E. De Paepe, MSc[1,2], Alberto Ara, MSc[1,2,3], Clara Garcia-Gorro, PhD[1,2], Saül Martinez-Horta, PhD[4,5,6], Jesus Perez-Perez, MSc [4,5,6], Jaime Kulisevsky, PhD[4,5,6], Nadia Rodriguez-Dechicha, MSc [7], Irene Vaquer, MSc [7], Susana Subira, PhD[7,8], Matilde Calopa, PhD[9], Esteban Muñoz, PhD[10,11,12], Pilar Santacruz, MSc[10], Jesus Ruiz-Idiago,PhD[13,14], Celia Mareca, MSc[13], Ruth de Diego-Balaguer,PhD[1,2,3,4,15], Estela Camara, PhD[1,2,4*]

1 Cognition and Brain Plasticity Unit [Bellvitge Biomedical Research Institute – IDIBELL], 08097 L'Hospitalet de Llobregat, Barcelona, Spain.

2 Department of Cognition, Development and Education Psychology, Universitat de Barcelona, Barcelona, Spain.

3 Institute of Neurosciences, Universitat de Barcelona, Barcelona, Spain.

4 European Huntington's Disease Network.

5 Movement Disorders Unit, Dept of Neurology, Biomedical Research Institute Sant Pau (IIB-Sant Pau), Hospital de la Santa Creu i Sant Pau, Barcelona, Spain.

6 CIBERNED (Center for Networked Biomedical Research on Neurodegenerative Diseases), Carlos III Institute, Madrid, Spain.

7 Hestia Duran i Reynals. Hospital Duran i Reynals, Hospitalet de Llobregat (Barcelona), Spain.

8 Departament de Psicologia Clínica i de la Salut, Universitat Autònoma de Barcelona, Barcelona, Spain.

9 Movement Disorders Unit, Neurology Service, Hospital Universitari de Bellvitge, Barcelona, Spain.

10 Movement Disorders Unit, Neurology Service, Hospital Clínic, Barcelona, Spain.

11 IDIBAPS (Institut d'Investigacions Biomèdiques August Pi i Sunyer), Barcelona, Spain.

12 Facultat de Medicina, University of Barcelona, Barcelona, Spain.

13 Department of Psychiatry and Forensic Medicine, Universitat Autònoma de Barcelona.

14 Hospital Mare de Deu de la Mercè, Barcelona, Spain.

15 ICREA (Catalan Institute for Research and Advanced Studies), Barcelona, Spain.

*Corresponding author: Estela Camara

Cognition and Brain Plasticity Unit, IDIBELL (Institut d'Investigació Biomèdica de Bellvitge)

Feixa Larga S/N, 08907 L'Hospitalet de Llobregat (Barcelona), Spain

Telephone: +34 934020489

www.brainvitge.org

E-mail: ecamara@ub.edu

Keywords: apathy, Huntington's disease, individual differences, longitudinal, neurodegeneration, structural MRI

Conflict of interest: The authors report no competing interests.

Funding: This work was supported by the Instituto de Salud Carlos III, an agency of the Ministerio de Ciencia, Innovación y Universidades (MINECO), co-funded by FEDER funds/European Regional Development Fund (ERDF) – a Way to Build Europe (CP13/00225 and PI14/00834, to EC). This study was also funded by the Agencia Estatal de Investigación (AEI), an agency of MINECO, and co-funded by FEDER funds/European Regional Development Fund (ERDF) – a Way to Build Europe (BFU2017-87109-P, to RdD). We thank CERCA Programme/Generalitat de Catalunya for institutional support. ADP received support from the Fulbright Program.

Abbreviations: ACC = anterior cingulate cortex; BA = Brodmann area; CAP = standardized CAG-Age Product; GMV = gray matter volume; HD = Huntington's disease; MCC = middle cingulate cortex; MNI = Montreal Neurological Institute coordinates; PBA-s = Problem Behavior Assessment, short-form; ROI = region-of-interest; TIV = total intracranial volume; UHDRS-cogscore = Unified Huntington's Disease Rating Scale total cognitive score; UHDRS-TMS = Unified Huntington's Disease Rating Scale total motor score; VIF = variance inflation factor; VBM = voxel-based morphometry

Abstract

Background: Apathy, a common neuropsychiatric disturbance in Huntington's disease (HD), is sub-served by a complex neurobiological network. However, no study has yet employed a whole-brain approach to examine underlying regional vulnerabilities that may precipitate apathy changes over time. **Objectives:** To identify whole-brain gray matter volume (GMV) vulnerabilities that may predict longitudinal apathy development in HD. **Methods:** Forty-five HD individuals (31 female) were scanned and evaluated for apathy and other neuropsychiatric features using the short-Problem Behavior Assessment for a maximum total of six longitudinal visits (including baseline). In order to identify regions where changes in GMV may describe changes in apathy, we performed longitudinal voxel-based morphometry (VBM) on those 33 participants with an MRI scan on their second visit at 18±6mon follow-up (78 MRI datasets). We next employed a generalized linear mixed-effects model (N=45) to elucidate whether initial and specific GMV may predict apathy development over time. **Results:** Utilizing longitudinal VBM, we revealed a relationship between increases in apathy and specific GMV atrophy in the right middle cingulate cortex (MCC). Furthermore, vulnerability in the right MCC volume at baseline successfully predicted the severity and progression of apathy over time. **Conclusions:** This study highlights that individual differences in apathy in HD may be explained by variability in atrophy and initial vulnerabilities in the right MCC, a region implicated in action-initiation. These findings thus serve to facilitate the prediction of an apathetic profile, permitting targeted, time-sensitive interventions in neurodegenerative disease with potential implications in otherwise healthy populations.

1. Introduction

Huntington's disease (HD) is an inherited neurodegenerative disorder that typically manifests in mid-adulthood and is caused by a cytosine-adenine-guanine polyglutamine expansion in the *HTT* gene(1,2). Gray matter loss begins in the neostriatum before extending into the cingulate, pre-central and prefrontal regions as well as occipital, parietal, and temporal cortices(3,4), with the rate of atrophy being most pronounced in the basal ganglia(5). This widespread degeneration results in a triad of progressive symptoms, including motor dysfunction, cognitive deficits, and neuropsychiatric disturbances such as apathy.

Apathy represents the most common neuropsychiatric feature in HD, occurring at a prevalence of 46-76% across premotor manifest and motor manifest HD individuals(6). As such, apathy constitutes a significant burden on the quality of life of patients and caregivers(7,8), impacting autonomy and social life. Additionally, unlike other common neuropsychiatric signs in HD, such as depression(9,10), apathy has been shown to closely track disease progression in cognitive and functional decline(5,11–14), although this positive coupling is not always reported(15,16).

When considering the underlying brain correlates of apathy in HD, recent studies have revealed that apathy is sub-served by a complex organization of subcortical and cortical regions that span cognitive and limbic territories. In particular, higher apathy severity has been associated with widespread neurobiological changes across imaging modalities, including gray matter volume (GMV) atrophy(17), reduced functional connectivity(18), and impaired white matter microstructure(19,20). While such cross-sectional studies shed

light on potential therapeutic targets for apathy in HD, their applicability in delineating longitudinal changes in a progressive neurodegenerative disorder is limited.

However, despite this need, few current studies examine the development of apathy in HD over time. Meanwhile, those longitudinal studies that do exist investigate the evolution of neuropsychiatric symptoms(5,9,15,16,21) in absence of neuroimaging data, or focus on a region-of-interest (ROI) based on *a priori* hypotheses of limited scope(14). It is therefore of crucial importance to conduct longitudinal analyses at the whole-brain level in order to establish whether atrophy across subcortical and cortical levels may predate, and thereby predict, apathy presentation. These specific patterns of brain alterations may, in turn, serve as targeted biomarkers that discern which individuals may be more susceptible to develop into a more neuropsychiatric clinical profile as the disease progresses(22). Such individual-level differentiation of disease profiles would thus provide an opportunity for early interventions that take advantage of a more personalized preventive and treatment regimen.

The goal of the present study is thus to examine the relationship between intra-individual changes in GMV and apathy, as opposed to depression and executive dysfunction, across the continuum of HD. Specifically, we performed longitudinal voxel-based morphometry (VBM) at the whole-brain level in order to identify regions where GMV atrophy may describe changes in apathy severity across two time points. We hypothesized that a greater loss of GMV would be associated with a larger increase in apathy severity over time. Subsequently, we employed a generalized linear mixed-effects model in order to elucidate whether initial and specific GMV vulnerability would successfully predict the longitudinal development of apathy at the individual level. We expected that regional vulnerability

(lower initial volumes) would be associated with higher rates of apathy presentation over time.

2. Methods and Materials

2.1. Participants

Participants' sociodemographic and clinical data are detailed in Table 1. Forty-five HD individuals underwent neuroimaging and apathy evaluation using the short-Problem Behavior Assessment (PBA-s) at baseline(23). While HD is clinically diagnosed based on motor onset, pathological, cognitive, and neuropsychiatric changes are often present long before motor symptoms(9,24). As such, and due to the fact that our main target was the neuropsychiatric profile, we studied the disease as a continuum. Therefore, while not all participants displayed motor symptoms (Table 1), each was genetically confirmed as a HD gene-carrier (43.91±3.04 CAG repeats).

In addition to the first (baseline) scan and assessment, all participants received neuropsychiatric evaluation using the PBA-s over a maximum total of six longitudinal visits (including baseline). Thirty-three participants also received an MRI scan on their second visit at 18±6 months follow-up. The generalized linear mixed-effects model analysis included all participants (N=45), with a mean number of 3.69±1.5 assessments and mean inter-assessment duration of 13.5±2 months.

No participants reported previous history of neurological disorder other than HD. The study was approved by the ethics committee of Bellvitge Hospital in accordance with the Helsinki Declaration of 1975, and all participants provided written informed consent.

2.2. Clinical evaluation

The evaluation of neuropsychiatric symptoms was conducted using the PBA-s, a semi-structured interview, administered in the presence of the main caregiver or other knowledgeable informant, which consists of eleven items: depressed mood, suicidal ideation, anxiety, irritability, angry or aggressive behavior, lack of initiative (apathy), preservative thinking or behavior, obsessive-compulsive behavior, paranoid/delusional thinking or behavior, hallucinations, and disoriented behavior. Scores are calculated as the product of frequency×severity (range: 0-16) for each symptom. An apathy score>2 was considered clinically relevant(24). As a control variable, non-apathetic neuropsychiatric disturbances were calculated as the sum of all ten additional (non-apathetic) items, allowing the examination of apathy as an independent neuropsychiatric symptom from the others. Similarly, non-depressive neuropsychiatric disturbances (all but depressed mood, suicidal ideation, and anxiety(3,25)) and the total PBA-s score were taken into account in models of depression and executive dysfunction, respectively.

In addition to the PBA-s, all participants were assessed with the Unified Huntington's Disease Rating Scale(26) for motor (UHDRS-TMS) and executive function (UHDRS-cogscore). UHDRS-TMS assesses the motor features of dysarthria, chorea, dystonia, gait, postural stability, and oculomotor function. UHDRS-cogscore includes the F-A-S test (phonetic verbal fluency) and the Symbol Digit Modalities Test (psychomotor speed) as well as the word-reading, color-naming, and interference components of the Stroop Test (processing speed, attention, and inhibitory control). A lower UHDRS-cogscore, in contrast to higher UHDRS-TMS and PBA-s scores, represents worse functioning. Total Functional Capacity was employed as a measure of independence in daily activities (range:

0 (total incapacity) - 13 (full capacity)). Lastly, the standardized CAG-Age Product (CAP) score, computed as CAP=100×age×(CAG–35.5)/627, was used as a measurement of HD state(27). All clinical assessments were carried out by neurologists or neuropsychologists specializing in movement disorders.

2.3. MRI acquisition and processing

MRI data were acquired through a 3T whole-body MRI scanner (Siemens Magnetom Trio; Hospital Clinic, Barcelona), using a 32-channel phased array head coil. Participants' images were acquired in the same scanner at both time points using the same acquisition protocol. Specifically, structural images comprised a conventional high-resolution 3D T1 image (magnetization-prepared rapid-acquisition gradient echo sequence), 208 sagittal slices, TR=1970ms, TE=2.34ms, TI=1050ms, flip angle=9º, FOV=256mm, 1mm isotropic voxel with no gap between slices.

2.4. Data analysis

2.4.1. Sociodemographic and clinical data

Statistical analyses of group demographics were performed in SPSS (v.25, SPSS Inc., Chicago, USA). In order to evaluate the potential of apathy to relate with HD state, we used univariate Spearman correlations of PBA-s apathy scores with CAP at baseline.

2.4.2 Voxel-based morphometry of T-1 weighted images

We carried out morphometric analysis using the longitudinal processing pipelines implemented in CAT12 toolbox (http://dbm.neuro.uni-jena.de/cat/) and SPM12 software

package (Welcome Department of Imaging Neuroscience Group, London, UK) running on MATLAB (v17.a, Mathworks, Natick, MA).

Specifically, preprocessing for the longitudinal data considered the characteristics of intra-subject analysis by the registration of the second image to the baseline image, and a subject-specific mean image was created from the realigned images and used as a reference for the realignment of both time points. Realigned images were segmented, corrected for signal inhomogeneity and normalized using the Diffeomorphic Anatomic Registration Through Exponentiated Lie algebra algorithm (DARTEL). Then, the corresponding normalization parameters were applied to the segmented gray matter images of both time points. Resulting gray matter normalized images were modulated by their Jacobian determinants and spatially smoothed (FWHM=8mm), allowing direct comparison of regional differences in gray matter volume(28). Finally, images were visually inspected.

The longitudinal smoothed GMV images were entered into a paired t-test in order to examine the effect of individual-level changes in GMV on changes in apathy between two time points. Time between scans (days), CAP scores, and non-apathetic neuropsychiatric disturbances were entered into the model as covariates of no interest. Explicit absolute masking with a threshold of 0.2 was applied in model selection (i.e., including only voxels with>20% probability of being gray matter) to more selectively distinguish GMV boundaries(29,30). Significant results were identified at $P<0.001$ (uncorrected) and a threshold of $P<0.05$ applied at cluster-level, with a minimum cluster size of 100 contiguous voxels. To test the specificity of the revealed region of atrophy to changes in apathy, the effects of PBA-s depression and UHDRS-cogscore were similarly evaluated through separate paired t-tests, including, as an explicit binary mask, the ROI volume in which we

observed longitudinal difference in apathy.

2.4.3. Generalized linear mixed-effects models

In order to study whether vulnerability in a specific ROI was predictive of longitudinal apathy development, as compared with depressive and executive functional outcomes, we implemented generalized linear mixed-effects models in R (v.3.5.1, R Foundation for Statistical Computing, Vienna, Austria). Generalized linear mixed-effects models provide greater flexibility in longitudinal analysis and are well suited for patient populations, as they allow for a different number of observations for each subject and non-equal intervals between assessments(31). Such models have previously been implemented in the study of HD(32–35).

In the primary set of models, longitudinal PBA-s apathy scores (maximum of six) were the outcome (dependent) variable. Besides time in days (accumulative, from the first to the final visit), the predictor variable of interest was the ROI volume in which we observed longitudinal differences in the VBM analyses. This volume was subsequently extracted from baseline scans using the xjView toolbox (http://www.alivelearn.net/xjview) and MATLAB in-house code (MATLAB R2017a, MathWorks, Natick, MA), and finally adjusted for total intracranial volume (TIV) at baseline [ROI volume/TIV]. Longitudinal values for CAP and non-apathetic neuropsychiatric disturbances were included as control variables. Because apathy scores are operationalized as counts, the dependent variable was assumed to follow a Poisson distribution, with the logarithmic link function used to map out predictions. Subject-specific random effects were specified for baseline (intercept), and random slopes were modeled for time. Predictor and control variables were scaled using

the *scale* function in R(36). In order to improve the precision of intercept estimates, all participants were included in analyses.

The analytic strategy was to fit two models for the outcome variable of longitudinal apathy. Model 1.0, the null model, only included the predictor variable of time. Meanwhile, Model 1.1 additionally included baseline ROI volume, with an interaction term between baseline ROI volume and time (see Equation 1). In both models, scaled predictor and control variables satisfied the condition for low multicollinearity, possessing a variance inflation factor (VIF)<2 as determined by the *check_collinearity* function in R(37).

Model 1.1, the more complex of the two models, is explicitly defined for clarity. Suppose the outcome variable, longitudinal apathy, is denoted as y, time as t, the initial ROI volume as r, CAP as c, non-apathetic neuropsychiatric disturbances as p, and s as the subject. The statistical model can then be defined as

$$y = \boldsymbol{\alpha} + \beta_1 t + \beta_2 r + \beta_3 (t)(r) + \beta_4 c + \beta_5 p + e_s \quad (1)$$

where $\boldsymbol{\alpha}$ is the intercept, β_1 and β_2 are the main effects, β_3 are the effects of the interaction term between time and the ROI volume, β_4 and β_5 are the respective slope effects of the control covariates, and e_s is subject-specific random effects at the intercept.

Goodness of fit of the two models was evaluated using the likelihood ratio test along with a probability scaling of Akaike's information criteria weight (W). The criteria represent the relative likelihood, or quality, of the statistical model. W values are considered a global relative effect size measure(38,39) and range from 0 to 1 (closer to 1 indicating better relative fit).

The above framework was identical for models of depression (Model 2.0 and 2.1) and executive dysfunction (Model 3.0 and 3.1), with the exception of the outcome variable (PBA-s depression; UHDRS-cogscore) and neuropsychiatric disturbances variable (non-depressive neuropsychiatric disturbances; total PBA-s score). Lastly, two longitudinal generalized linear mixed-effects models were carried out to evaluate the association between apathy as the outcome variable, the scaled predictor variable being PBA-s depression in the first model and UHDRS-cogscore in the second model.

Due to the lack of apathy signs in twelve individuals (26.7%), we utilized the glmmTMB package to account for zero-inflation in the set of apathy models(40), where its application was statistically significant (P_{zi}<0.05), but not in models with outcome variables of depression and executive dysfunction. Zero-inflated models are designed to accommodate samples with a large number of zeros, in such a way that predictions are made considering the expected number of zeros under the current statistical process. Analysis code is available in Supplemental Information.

3. Results

3.1. Sociodemographic and clinical data

At the first (baseline) visit, PBA-s apathy levels ranged from 0-16, with an average of 4.28±5.0, with 47.8% of individuals manifesting clinical levels of apathy and 41.3% of individuals not expressing signs of apathy. Baseline apathy scores were found to significantly correlate with CAP (r_s=.381, P=.010, N=45), with a large effect size(41). When considering longitudinal data, 64.4% of individuals manifested clinical levels of apathy at some point throughout the course of the study, with only 26.7% not expressing

even mild signs of apathy. Baseline characteristics of the VBM analysis are displayed in Table S1. Longitudinal data from each participant are depicted in Figure S1.

3.2. VBM results

We first sought to examine the relationship between intra-individual changes in apathy severity and changes in GMV across two time points. Utilizing a whole-brain approach, we found that an increase in apathy was associated with a larger reduction in GMV specifically in the right middle cingulate cortex (MCC; BA24) (Figure 1). This relationship maintained significance both with (*cluster size*=259, *T*=4.63, *P*<0.001, MNI [*x*=9, *y*=8, *z*=35]) and without (*cluster size*=286, *T*=4.50, *P*<0.001, MNI [*x*=14, *y*=2, *z*=41]) controlling the CAP score as a proxy measure for disease state after correction for multiple comparisons at cluster-level. In *post-hoc* analysis controlling for non-apathetic neuropsychiatric disturbances, small volume correction (sphere radius=12mm; *P*=0.005) centered on the right MCC showed the ROI to maintain the direction of the effect (*T*=2.89, *P*=0.004, MNI [*x*=9, *y*=9, *z*=33]). Furthermore, this right MCC effect was maintained at whole-brain level when assessed in premanifest (*N*=15) individuals only (*cluster size*=320, *T*=4.89, *P*<0.001, MNI [*x*=8, *y*=5, *z*=30]), in addition to the cuneus and inferior occipital lobe (Table S2). Meanwhile, no significant effects were found in separate control analyses between the right MCC with depression and UHDRS-cogscore, when assessed with the ROI mask across all HD participants.

3.3. Generalized linear mixed-effects models

When examining the likelihood ratio test between the two apathy models, it was found that Model 1.1 (that with an interaction term between baseline MCC and time) was of superior

likelihood, demonstrating a statistically significant better fit than the null Model 1.0 ($\chi^2(2)=6.5$, $P=0.040$). This finding was further exemplified through the superior Akaike's information criteria weight for Model 1.1 ($W=0.773$) when compared to the null ($W=0.227$).

When evaluating the significance of individual variables (Table 2), the interaction term of Model 1.1 illustrates that a small MCC volume is capable of predicting how apathy levels change longitudinally. Specifically, the negative β Estimate value indicates that, as apathy increases over time, those with larger initial MCC volumes experience a slower rate of change in apathy, demonstrating a plateau or even a slight decrease in apathy. On the other hand, those with a smaller initial MCC volume increased in apathy, and at a faster rate (Figure 2).

In follow-up models of PBA-s depression and UHDRS-cogscore, the inclusion of the interaction between initial MCC volume and time resulted in a statistically superior model predictive of executive dysfunction (Model 3; $\chi^2(2)=9.45$, $P=0.009$), but not depression (Model 2; $\chi^2(2)=2.29$, $P=0.318$), compared to their respective null models (Table 2). Lastly, longitudinal UHDRS-cogscore, but not depression, was significantly associated with apathy development (Table S3).

4. Discussion

The goal of the present study was to investigate the longitudinal development of apathy, compared with depressive and executive functional outcomes, as predicted by atrophy and initial vulnerability in regional GMV. Utilizing VBM, we revealed that specific GMV atrophy in the right MCC (BA24) was related to increases in apathy severity over time, but

not depression or executive dysfunction. Furthermore, vulnerability in the MCC volume at baseline successfully predicted the longitudinal severity and progression of apathy, even after controlling for CAP, a proxy of disease state, as elucidated through the generalized linear mixed-effects models. In brief, the interaction term in Model 1.1 highlights that initial vulnerability (smaller volume) in the MCC may be predictive of those individuals who were more likely to develop apathy or experience worsening apathy at a future point in time. By extension, initial MCC volume additionally informed a prognosis of worsening executive functional outcomes.

Previously known as the dorsal anterior cingulate cortex (ACC)(42), the MCC has long been implicated in goal-directed behaviors (i.e., those that are disrupted in apathy), thus serving as a neurological interface between motivation and action execution, especially for effortful actions(43–45). Indeed, damage to this region has been confirmed to play a role in the manifestation of apathy(46,47) and abulia(48) across a range of clinical neurological disorders. Moreover, previous studies postulate that the MCC may form a part of a medial frontostriatal apathy circuit innervating the ventral striatum and extending to the orbitofrontal cortex(43,49–52). Damage to this MCC circuit at either the subcortical or cortical level may therefore directly contribute to the development of emotional, cognitive, and behavioral inactivity and a loss of spontaneity(44) as well as impaired decision-making(45).

Examining the frontostriatal circuits implicated in apathy sheds light on the characteristic complex of both cortical and subcortical territories involved in apathy in HD. In the present study, atrophy in such subcortical regions was not significantly associated with increased apathy over time. This may be due to the distinct rates of atrophy in the basal ganglia

compared with cortical regions in HD, the latter of which may more closely parallel the rate of change in apathy. Indeed, examining GMV cross-sectionally corroborated an association between apathy and both subcortical and cortical territories (see Figure S2; Table S4), wherein lower GMV was associated with higher apathy severity. This pattern of limbic and cognitive regions closely mirrored those found in past literature(17). Specifically, across both structural and functional modalities, neural correlates have been shown to include the medial orbitofrontal cortex, supplementary motor area, cingulate, caudate, and ventral striatum, or connectivity between such regions(17–20), with a disputed involvement of the thalamus(12,47). This complex interplay may be due to the multidimensional, transdiagnostic nature of apathy as composed of apathy subdomains, each represented by a discrete underlying neurobiological framework(20,49,54).

All in all, the MCC (BA24) has been associated with apathy severity in both healthy and neurologically impaired populations(46,49,55). For example, apathy in otherwise healthy individuals has been related with decreased salience-related processing in ACC(56) as well as a greater recruitment of ACC and supplementary motor area, two neural systems involved in action anticipation(57). One case study reported aberrant functional connectivity in the dorsal ACC in patients with abulia compared to controls, even in the absence of structural damage(58). When examining cross-sectional gray matter atrophy specifically, reduced gray matter density or volume in the middle cingulate gyrus has been linked to more severe apathy in frontotemporal dementia(59), Parkinson's disease(60), and Alzheimer's disease(61,62) in addition to HD(17), bilaterally or predominantly in the right hemisphere.

The MCC (BA24) bears distinct structural and functional connectivity from the more rostral/ventral ACC(42,63). In short, while ACC connectivity extends to regions involved in emotion, autonomic function, and reward processing, the MCC shares extensive connections specifically with cognitive- and motor-related cortical regions, including dorsal prefrontal and premotor cortices(64). In the current study, the fact that apathy development in HD is specifically represented by atrophy in the MCC, as opposed to the ACC, may explain the differential expression of apathy domains in this patient population(20). Lastly, it is interesting to note that MCC atrophy was not indicative of changes in depression, a disorder often associated with the more rostral/ventral ACC(65).

Functionally, the MCC is activated during cognitive and motor-related tasks. This is exemplified in effort-based response-selection and execution, such as when action selection is directed by reward anticipation and reinforcement(58,59). Such effort-based decision-making is compromised in individuals with apathy(67,68). Ultimately, the present results underscore the notion that disruption to the integrative functionality of the MCC may sub-serve not only the prognosis of apathy and executive dysfunction in HD, but also the coevolution of these two devastating clinical features.

In this vein, both HD patients and caregivers describe cognitive and neuropsychiatric symptoms as imposing a greater burden on functional capacity and quality of life than motor dysfunction, with no effective treatment for cognitive decline and apathy currently available(5,69). Furthermore, 39.2% of gene-carriers may present cognitive and/or neuropsychiatric disturbances in the absence of motor symptoms(70), with neuropsychiatric aspects appearing up to ten years prior to clinical diagnosis by motor onset(24,71). Specifically, increased apathy severity has long been associated with a

deterioration of higher order cognitive functions in both healthy aging and neurologically impaired populations, particularly in tasks involving initiation processes and task switching(68,72–76). More recently, apathy was found to predict rates of cognitive decline in premanifest HD individuals(77). Neurobiologically, both apathy and executive dysfunction are related with lesions in frontal cortico-striatal circuitry(50,78). In light of this, future investigation focusing on the interaction between the MCC, apathy, and executive function would be especially relevant in the elucidation of distinct profiles of HD, where the presentation of motor, cognitive, and neuropsychiatric symptoms is heterogeneous at the individual level(22).

The present study is not without limitations. First, it is important to note that the sample is not representative of all HD gene-carriers. In particular, the VBM analysis includes only those participants willing to take part in a longitudinal study. In order to minimize this effect of potentially non-random attrition, all longitudinal and cross-sectional data were incorporated in the generalized linear mixed-effects models. As such, while the models included a maximum total of six apathy assessments, a subset of individuals received only one evaluation. Future studies that have the potential to link longitudinal evaluation of neuropsychiatric signs and neural correlates may be more sensitive to detect patterns of atrophy that predate subtle changes in apathy. Indeed, latent difference score models have demonstrated that recent brain changes may indicate the advent of cognitive decline in a coupled-over-time manner(79,80), exemplifying the value of repeated measures in both neuroimaging and behavioral evaluations when evaluating time-dependency relationships. In parallel, complementing longitudinal volumetric neuroimaging with other structural,

morphometric, or functional protocols is also of interest, especially as distinct imaging modalities may be more sensitive to different neural substrates(81).

In line with this limitation, and as previously denoted, the longitudinal, whole-brain analysis of the present study did not expose other elements of the medial frontostriatal apathy circuit beyond the MCC (i.e., orbitofrontal cortex, ventral striatum). As such, while these findings elucidate the vulnerability of the MCC as a specific predictor of apathy development over time, this study by no means simplifies the picture of apathy in HD; rather, it serves to highlight the existing gaps in the study of this multidimensional, transdiagnostic symptom and syndrome. In future studies, the evaluation of apathy subdomains may prove to be more sensitive to disentangling the swath of neural correlates that represent apathy. Such work would be valuable in assessing whether the MCC and other regions are implicated in both neurologically impaired and otherwise healthy individuals in which apathy is prevalent.

Additionally, while not the focus of the study, it should be noted that the UHDRS-cogscore is a limited estimate of cognition, specific to processing speed and executive function (82). Furthermore, all UHDRS components are sensitive to age-related decline. For this reason, corrections for CAP were included in all analyses as control covariates.

Lastly, it is important to note that the apathy models accounted for zero-inflation. This relates to the 26.7% (12/45) of individuals that did not develop even mild, sub-clinical signs of apathy over the course of the study. This absence of apathy may be explained by other life factors that protect these individuals from developing apathy, irrespective of their initial MCC size.

This paper provides a whole-brain longitudinal evaluation of the relationship between changes in apathy and atrophy of underlying brain correlates in HD, as such filling a noted gap in the literature. Not only do these findings reveal that a reduction in the MCC volume is significantly related to an increase in apathy severity in HD at the individual level; we also highlighted that initial vulnerabilities in the MCC may be predictive of those individuals who are predisposed to develop apathy and accompanying executive dysfunction at a faster rate in time. As such, this study opens a door to the incipient detection of those individuals who may be prone to develop a more apathetic neuropsychiatric profile in the future. In this case, the personalized management of apathy during an earlier, optimal window may be initiated, including both pharmacological and behavioral interventions. Ultimately, this study may serve as a model for the anticipative evaluation of common neuropsychiatric features in HD, with potential applications to other neurodegenerative diseases as well as otherwise healthy populations suffering from apathy.

Acknowledgments

The authors are grateful to the patients and their families for their participation in this project. We would also like to thank Dr. Alexis Pérez Bellido for the discussion of generalized linear mixed-effects models.

Authors' roles

Audrey E De Paepe: 1C, 2A, 2B, 3A, 3B

Alberto Ara: 2A, 2B, 2C, 3B

Clara Garcia-Gorro: 1B, 1C, 3B

Saül Martinez-Horta: 1C, 3B

Jesus Perez-Perez: 1C, 3B

Jaime Kulisevsky: 1C, 3B

Nadia Rodriguez-Dechicha: 1C, 3B

Irene Vaquer: 1C, 3B

Susana Subira: 1C, 3B

Matilde Calopa: 1C, 3B

Esteban Muñoz: 1C, 3B

Pilar Santacruz: 1C, 3B

Jesus Ruiz-Idiago: 1C, 3B

Celia Mareca: 1C, 3B

Ruth de Diego-Balaguer: 1A, 1B, 3B

Estela Camara: 1A, 1B, 1C, 2A, 2C, 3B

Financial disclosures

Audrey E De Paepe: None

Alberto Ara: None

Clara Garcia-Gorro: None

Saül Martinez-Horta: None

Jesus Perez-Perez: None

Jaime Kulisevsky: None

Nadia Rodriguez-Dechicha: None

Irene Vaquer: None

Susana Subira: None

Matilde Calopa: None

Esteban Muñoz: None

Pilar Santacruz: None

Jesus Ruiz-Idiago: None

Celia Mareca: None

Ruth de Diego-Balaguer: None

Estela Camara: None

References

1. MacDonald ME, Ambrose CM, Duyao MP, Myers RH, Lin C, Srinidhi L, et al. A novel gene containing a trinucleotide repeat that is expanded and unstable on Huntington's disease chromosomes. Cell. 1993 Mar 26;72(6):971–83.

2. Langbehn DR, Hayden M, Paulsen JS. CAG-Repeat Length and the Age of Onset in Huntington Disease (HD): A Review and Validation Study of Statistical Approaches. Am J Med Genet Part B Neuropsychiatr Genet Off Publ Int Soc Psychiatr Genet. 2010 Mar 5;153B(2):397–408.

3. Tabrizi SJ, Langbehn DR, Leavitt BR, Roos RA, Durr A, Craufurd D, et al. Biological and clinical manifestations of Huntington's disease in the longitudinal TRACK-HD study: cross-sectional analysis of baseline data. Lancet Neurol. 2009;8(9):791–801.

4. Waldvogel HJ, Kim EH, Tippett LJ, Vonsattel J-PG, Faull RL. The Neuropathology of Huntington's Disease. In: Nguyen HHP, Cenci MA, editors. Behavioral Neurobiology of Huntington's Disease and Parkinson's Disease [Internet]. Berlin, Heidelberg: Springer Berlin Heidelberg; 2014 [cited 2017 Nov 4]. p. 33–80. Available from: http://link.springer.com/10.1007/7854_2014_354

5. Tabrizi SJ, Scahill RI, Owen G, Durr A, Leavitt BR, Roos RA, et al. Predictors of phenotypic progression and disease onset in premanifest and early-stage Huntington's disease in the TRACK-HD study: analysis of 36-month observational data. Lancet Neurol. 2013 Jul;12(7):637–49.

6. Camacho M, Barker RA, Mason SL. Apathy in Huntington's Disease: A Review of the Current Conceptualization. J Alzheimer's Dis Park. 2018;08(02).

7. Chase TN. Apathy in Neuropsychiatric Disease: Diagnosis, Pathophysiology, and Treatment. Neurotox Res. 2011 Feb;19(2):266–78.

8. Paoli R, Botturi A, Ciammola A, Silani V, Prunas C, Lucchiari C, et al. Neuropsychiatric Burden in Huntington's Disease. Brain Sci. 2017 Jun 16;7(6):67.

9. Thompson J, Harris J, Sollom A, Stopford C, Howard E, Snowden J, et al. Longitudinal evaluation of neuropsychiatric symptoms in Huntington's disease. J Neuropsychiatry Clin Neurosci. 2012;24:53–60.

10. Naarding P, Janzing JG, Eling P, van der Werf S, Kremer B. Apathy is not depression in Huntington's disease. J Neuropsychiatry Clin Neurosci. 2009;21(3):266–70.

11. Kingma EM, van Duijn E, Timman R, van der Mast RC, Roos RAC. Behavioural problems in Huntington's disease using the Problem Behaviours Assessment. Gen Hosp Psychiatry. 2008 Mar;30(2):155–61.

12. Thompson JC, Snowden JS, Craufurd D, Neary D. Behavior in Huntington's disease: dissociating cognition-based and mood-based changes. J Neuropsychiatry Clin Neurosci. 2002;14(1):37–43.

13. van Duijn E, Craufurd D, Hubers AAM, Giltay EJ, Bonelli R, Rickards H, et al. Neuropsychiatric symptoms in a European Huntington's disease cohort (REGISTRY). J Neurol Neurosurg Psychiatry. 2014 Dec;85(12):1411–8.

14. Baake V, Coppen EM, van Duijn E, Dumas EM, van den Bogaard SJA, Scahill RI, et al. Apathy and atrophy of subcortical brain structures in Huntington's disease: A two-year follow-up study. NeuroImage Clin. 2018;19:66–70.

15. van Duijn E, Reedeker N, Giltay EJ, Eindhoven D, Roos RAC, van der Mast RC. Course of Irritability, Depression and Apathy in Huntington's Disease in Relation to Motor Symptoms during a Two-Year Follow-Up Period. Neurodegener Dis [Internet]. 2013 [cited 2019 May 3]; Available from: https://www.karger.com/Article/FullText/343210

16. Mason S, Barker RA. Rating Apathy in Huntington's Disease: Patients and Companions Agree. J Huntingt Dis. 2015;4:49–59.

17. Martinez-Horta S, Perez-Perez J, Sampedro F, Pagonabarraga J, Horta-Barba A, Carceller-Sindreu M, et al. Structural and metabolic brain correlates of apathy in Huntington's disease: Apathy in Huntington's Disease. Mov Disord. 2018 Jul;33(7):1151–9.

18. McColgan P, Razi A, Gregory S, Seunarine KK, Durr A, A.C. Roos R, et al. Structural and functional brain network correlates of depressive symptoms in premanifest Huntington's disease: Depressive Symptoms in preHD. Hum Brain Mapp. 2017 Jun;38(6):2819–29.

19. Delmaire C, Dumas EM, Sharman MA, van den Bogaard SJA, Valabregue R, Jauffret C, et al. The structural correlates of functional deficits in early huntington's disease: Structural Correlates of Functional Deficits in HD. Hum Brain Mapp. 2013 Sep;34(9):2141–53.

20. De Paepe AE, Sierpowska J, Garcia-Gorro C, Martinez-Horta S, Perez-Perez J, Kulisevsky J, et al. White matter cortico-striatal tracts predict apathy subtypes in Huntington's disease. NeuroImage Clin. 2019;24:101965.

21. Reedeker N, Bouwens J, van Duijn E, Giltay EJ, Roos RAC, van der Mast RC. Incidence, Course, and Predictors of Apathy in Huntington's Disease: A Two-Year Prospective Study. J Neuropsychiatry Clin Neurosci. 2011 Sep;23(4):434.

22. Garcia-Gorro C, Llera A, Martinez-Horta S, Perez-Perez J, Kulisevsky J, Rodriguez-Dechicha N, et al. Specific patterns of brain alterations underlie distinct clinical profiles in Huntington's disease. NeuroImage Clin. 2019;23:101900.

23. Callaghan J, Stopford C, Arran N, Boisse M-F, Coleman A, Santos RD, et al. Reliability and Factor Structure of the Short Problem Behaviors Assessment for Huntington's Disease (PBA-s) in the TRACK-HD and REGISTRY studies. J Neuropsychiatry Clin Neurosci. 2015 Jan;27(1):59–64.

24. Martinez-Horta S, Perez-Perez J, van Duijn E, Fernandez-Bobadilla R, Carceller M, Pagonabarraga J, et al. Neuropsychiatric symptoms are very common in premanifest and early stage Huntington's Disease. Parkinsonism Relat Disord. 2016 Feb;30:58–64.

25. Craufurd D, Thompson JC, Snowden JS. Behavioral changes in Huntington Disease. Neuropsychiatry Neuropsychol Behav Neurol. 2001 Dec;14(4):219–26.

26. Huntington Study Group. Unified Huntington's disease rating scale: Reliability and consistency. Mov Disord. 1996 Mar 1;11(2):136–42.

27. Ross CA, Aylward EH, Wild EJ, Langbehn DR, Long JD, Warner JH, et al. Huntington disease: natural history, biomarkers and prospects for therapeutics. Nat Rev Neurol. 2014 Apr;10(4):204–16.

28. Mechelli A, Friston KJ, Frackowiak RS, Price CJ. Structural Covariance in the Human Cortex. J Neurosci. 2005 Sep;25(36):8303–10.

29. Ashburner J. VBM Tutorial [Internet]. 2010. Available from: http://www.fil.ion.ucl.ac.uk/~john/misc/ VBMclass10.pdf

30. James CE, Oechslin MS, Van De Ville D, Hauert C-A, Descloux C, Lazeyras F. Musical training intensity yields opposite effects on grey matter density in cognitive versus sensorimotor networks. Brain Struct Funct. 2014 Jan;219(1):353–66.

31. Gibbons RD, Hedeker D, DuToit S. Advances in Analysis of Longitudinal Data. Annu Rev Clin Psychol. 2010 Apr 27;6:79–107.

32. Bonner-Jackson A, Long JD, Westervelt H, Tremont G, Aylward E, Paulsen JS, et al. Cognitive Reserve and Brain Reserve in Prodromal Huntington's Disease. J Int Neuropsychol Soc. 2013 Aug;19(07):739–50.

33. Odish OFF, Leemans A, Reijntjes RHAM, van den Bogaard SJA, Dumas EM, Wolterbeek R, et al. Microstructural brain abnormalities in Huntington's disease: A two-year follow-up: Microstructural Brain Abnormalities in HD. Hum Brain Mapp. 2015 Jun;36(6):2061–74.

34. Harrington DL, Long JD, Durgerian S, Mourany L, Koenig K, Bonner-Jackson A, et al. Cross-sectional and longitudinal multimodal structural imaging in prodromal Huntington's disease: Structure Imaging in Prodromal HD. Mov Disord. 2016 Nov;31(11):1664–75.

35. de Diego-Balaguer R, Schramm C, Rebeix I, Dupoux E, Durr A, Brice A, et al. COMT Val158Met Polymorphism Modulates Huntington's Disease Progression. Blum D, editor. PLOS ONE. 2016 Sep 22;11(9):e0161106.

36. Becker RA, Chambers JM, Wilks AR. The New S Language. Wadsworth & Brooks/Cole; 1988.

37. Lüdecke D, Makowski D, Waggoner P. performance: Assessment of Regression Models Performance. 2019; Available from: https://easystats.github.io/performance/

38. Burnham K, Anderson D. Model Selection and Multimodal Inference. New York: Springer; 2002.

39. Long J. Data Analysis for Behavioral Sciences Using R. Thousand Oaks, CA: Sage Publications Inc.; 2011.

40. Brooks ME, Kristensen K, Benthem KJ van, Magnusson A, Berg CW, Nielsen A, et al. glmmTMB Balances Speed and Flexibility Among Packages for Zero-inflated Generalized Linear Mixed Modeling. R J. 2017;9(2):378–400.

41. Gignac GE, Szodorai ET. Effect size guidelines for individual differences researchers. Personal Individ Differ. 2016 Nov;102:74–8.

42. Vogt BA. Midcingulate cortex: Structure, connections, homologies, functions and diseases. J Chem Neuroanat. 2016 Jul;74:28–46.

43. Mega MS, Cummings JL, Salloway S, Malloy P. The limbic system: an anatomic, phylogenetic, and clinical perspective. J Neuropsychiatry Clin Neurosci. 1997;9(3):315–30.

44. Allman JM, Hakeem A, Erwin JM, Nimchinsky E, Hof P. The Anterior Cingulate Cortex: The Evolution of an Interface between Emotion and Cognition. Ann N Y Acad Sci. 2006 Jan 25;935(1):107–17.

45. Theleritis C, Politis A, Siarkos K, Lyketsos CG. A review of neuroimaging findings of apathy in Alzheimer's disease. Int Psychogeriatr. 2014 Feb;26(2):195–207.

46. Kos C, van Tol M-J, Marsman J-BC, Knegtering H, Aleman A. Neural correlates of apathy in patients with neurodegenerative disorders, acquired brain injury, and psychiatric disorders. Neurosci Biobehav Rev. 2016 Oct;69:381–401.

47. Le Heron C, Apps. MAJ, Husain M. The anatomy of apathy: A neurocognitive framework for amotivated behaviour. Neuropsychologia. 2018;118:54–67.

48. Lavretsky H, Zheng L, Weiner MW, Mungas D, Reed B, Kramer JH, et al. The MRI brain correlates of depressed mood, anhedonia, apathy, and anergia in older adults with and without cognitive impairment or dementia. Int J Geriatr Psychiatry. 2008 Oct;23(10):1040–50.

49. Levy R, Dubois B. Apathy and the Functional Anatomy of the Prefrontal Cortex-Basal Ganglia Circuits. Cereb Cortex. 2006 Jul;16(7):916–28.

50. Bonelli RM, Cummings JL. Frontal-subcortical circuitry and behavior. Dialogues Clin Neurosci. 2007;9(2):141.

51. Guimarães HC, Levy R, Teixeira AL, Beato RG, Caramelli P. Neurobiology of apathy in Alzheimer's disease. Arq Neuropsiquiatr. 2008 Jun;66(2b):436–43.

52. Robert PH, Mulin E, Malléa P, David R. REVIEW: Apathy Diagnosis, Assessment, and Treatment in Alzheimer's Disease. CNS Neurosci Ther. 2010 Sep 3;16(5):263–71.

53. Misiura MB, Ciarochi J, Vaidya J, Bockholt J, Johnson HJ, Calhoun VD, et al. Apathy Is Related to Cognitive Control and Striatum Volumes in Prodromal Huntington's Disease. J Int Neuropsychol Soc. 2019 Feb 26;1–8.

54. Pagonabarraga J, Kulisevsky J, Strafella AP, Krack P. Apathy in Parkinson's disease: clinical features, neural substrates, diagnosis, and treatment. Lancet Neurol. 2015 May;14(5):518–31.

55. Moretti R, Signori R. Neural Correlates for Apathy: Frontal-Prefrontal and Parietal Cortical- Subcortical Circuits. Front Aging Neurosci [Internet]. 2016 Dec 9 [cited 2018 Dec 3];8. Available from: http://journal.frontiersin.org/article/10.3389/fnagi.2016.00289/full

56. Onoda K, Yamaguchi S. Dissociative contributions of the anterior cingulate cortex to apathy and depression: Topological evidence from resting-state functional MRI. Neuropsychologia. 2015 Oct;77:10–8.

57. Bonnelle V, Manohar S, Behrens T, Husain M. Individual Differences in Premotor Brain Systems Underlie Behavioral Apathy. Cereb Cortex. 2016;bhv247.

58. Siegel JS, Snyder AZ, Metcalf NV, Fucetola RP, Hacker CD, Shimony JS, et al. The circuitry of abulia: Insights from functional connectivity MRI. NeuroImage Clin. 2014;6:320–6.

59. Massimo L, Powers C, Moore P, Vesely L, Avants B, Gee J, et al. Neuroanatomy of Apathy and Disinhibition in Frontotemporal Lobar Degeneration. Dement Geriatr Cogn Disord. 2009;27(1):96–104.

60. Reijnders JSAM, Scholtissen B, Weber WEJ, Aalten P, Verhey FRJ, Leentjens AFG. Neuroanatomical correlates of apathy in Parkinson's disease: A magnetic resonance imaging study using voxel-based morphometry. Mov Disord Off J Mov Disord Soc. 2010 Oct 30;25(14):2318–25.

61. Apostolova LG, Akopyan GG, Partiali N, Steiner CA, Dutton RA, Hayashi KM, et al. Structural Correlates of Apathy in Alzheimer's Disease. Dement Geriatr Cogn Disord. 2007;24(2):91–7.

62. Bruen PD, McGeown WJ, Shanks MF, Venneri A. Neuroanatomical correlates of neuropsychiatric symptoms in Alzheimer's disease. Brain J Neurol. 2008 Sep;131(Pt 9):2455–63.

63. Stevens FL. Anterior Cingulate Cortex: Unique Role in Cognition and Emotion. J Neuropsychiatry Clin Neurosci. 2011;6.

64. Beckmann M, Johansen-Berg H, Rushworth MFS. Connectivity-Based Parcellation of Human Cingulate Cortex and Its Relation to Functional Specialization. J Neurosci. 2009 Jan 28;29(4):1175–90.

65. Koolschijn PCMP, Haren NEM van, Lensvelt- Mulders GJLM, Pol HEH, Kahn RS. Brain volume abnormalities in major depressive disorder: A meta-analysis of magnetic resonance imaging studies. Hum Brain Mapp. 2009;30(11):3719–35.

66. Rushworth MFS, Behrens TEJ, Rudebeck PH, Walton ME. Contrasting roles for cingulate and orbitofrontal cortex in decisions and social behaviour. Trends Cogn Sci. 2007 Apr;11(4):168–76.

67. Kurniawan IT, Guitart-Masip M, Dolan RJ. Dopamine and Effort-Based Decision Making. Front Neurosci [Internet]. 2011 Jun 21 [cited 2019 May 14];5. Available from: https://www.ncbi.nlm.nih.gov/pmc/articles/PMC3122071/

68. Le Heron C, Manohar S, Plant O, Muhammed K, Griffanti L, Nemeth A, et al. Dysfunctional effort-based decision-making underlies apathy in genetic cerebral small vessel disease. Brain [Internet]. 2018 Oct 20 [cited 2018 Oct 26]; Available from: https://academic.oup.com/brain/advance-article/doi/10.1093/brain/awy257/5139779

69. Eddy CM, Parkinson EG, Rickards HE. Changes in mental state and behaviour in Huntington's disease. Lancet Psychiatry. 2016 Nov;3(11):1079–86.

70. Vinther-Jensen T, Larsen IU, Hjermind LE, Budtz-Jørgensen E, Nielsen TT, Nørremølle A, et al. A clinical classification acknowledging neuropsychiatric and cognitive impairment in Huntington's disease. Orphanet J Rare Dis. 2014 Dec;9(1):114.

71. Duff K, Paulsen JS, Beglinger LJ, Langbehn DR, Stout JC. Psychiatric Symptoms in Huntington's Disease before Diagnosis: The Predict-HD Study. Biol Psychiatry. 2007 Dec 15;62(12):1341–6.

72. Zgaljardic DJ, Borod JC, Foldi NS, Rocco M, Mattis PJ, Gordon MF, et al. Relationship Between Self-reported Apathy and Executive Dysfunction in Nondemented Patients With Parkinson Disease. Cogn Behav Neurol Off J Soc Behav Cogn Neurol. 2007 Sep;20(3):184–92.

73. Varanese S, Perfetti B, Ghilardi MF, Di Rocco A. Apathy, but Not Depression, Reflects Inefficient Cognitive Strategies in Parkinson's Disease. Aleman A, editor. PLoS ONE. 2011 Mar 18;6(3):e17846.

74. Sinha N, Manohar S, Husain M. Impulsivity and apathy in Parkinson's disease. J Neuropsychol. 2013 Sep;7(2):255–83.

75. Meyer A, Zimmermann R, Gschwandtner U, Hatz F, Bousleiman H, Schwarz N, et al. Apathy in Parkinson's disease is related to executive function, gender and age but not to depression. Front Aging Neurosci [Internet]. 2015 Jan 15 [cited 2019 Feb 6];6. Available from: http://journal.frontiersin.org/article/10.3389/fnagi.2014.00350/abstract

76. Kawagoe T, Onoda K, Yamaguchi S. Apathy and Executive Function in Healthy Elderly—Resting State fMRI Study. Front Aging Neurosci. 2017 May 9;9:124.

77. Andrews SC, Langbehn DR, Craufurd D, Durr A, Leavitt BR, Roos RA, et al. Apathy predicts rate of cognitive decline over 24 months in premanifest Huntington's disease. Psychol Med. 2020;1–7.

78. Leh SE, Petrides M, Strafella AP. The Neural Circuitry of Executive Functions in Healthy Subjects and Parkinson's Disease. Neuropsychopharmacology. 2010 Jan;35(1):70–85.

79. McArdle JJ, Hamgami F, Jones K, Jolesz F, Kikinis R, Spiro A, et al. Structural Modeling of Dynamic Changes in Memory and Brain Structure Using Longitudinal Data From the Normative Aging Study. J Gerontol B Psychol Sci Soc Sci. 2004 Nov 1;59(6):P294–304.

80. Grimm KJ, An Y, McArdle JJ, Zonderman AB, Resnick SM. Recent Changes Leading to Subsequent Changes: Extensions of Multivariate Latent Difference Score Models. Struct Equ Model Multidiscip J. 2012 Apr 1;19(2):268–92.

81. Cercignani M, Bouyagoub S. Brain microstructure by multi-modal MRI: Is the whole greater than the sum of its parts? NeuroImage. 2018 Nov;182:117–27.

82. Toh EA, MacAskill MR, Dalrymple-Alford JC, Myall DJ, Livingston L, Macleod SA, et al. Comparison of cognitive and UHDRS measures in monitoring disease progression in Huntington's disease: a 12-month longitudinal study. Transl Neurodegener. 2014;3:15.

Figures

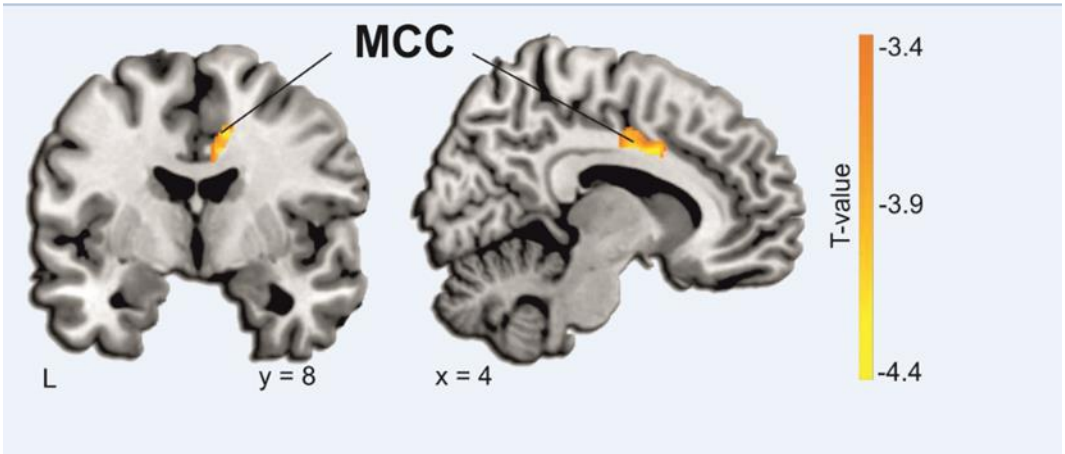

Figure 1. Specific gray matter atrophy in the right MCC relates with increasing apathy severity over time (18±6mon follow-up; cluster size=100; *P*<0.001). Slice position labeled in Montreal Neurological Institute coordinates. MCC=middle cingulate cortex; R=right.

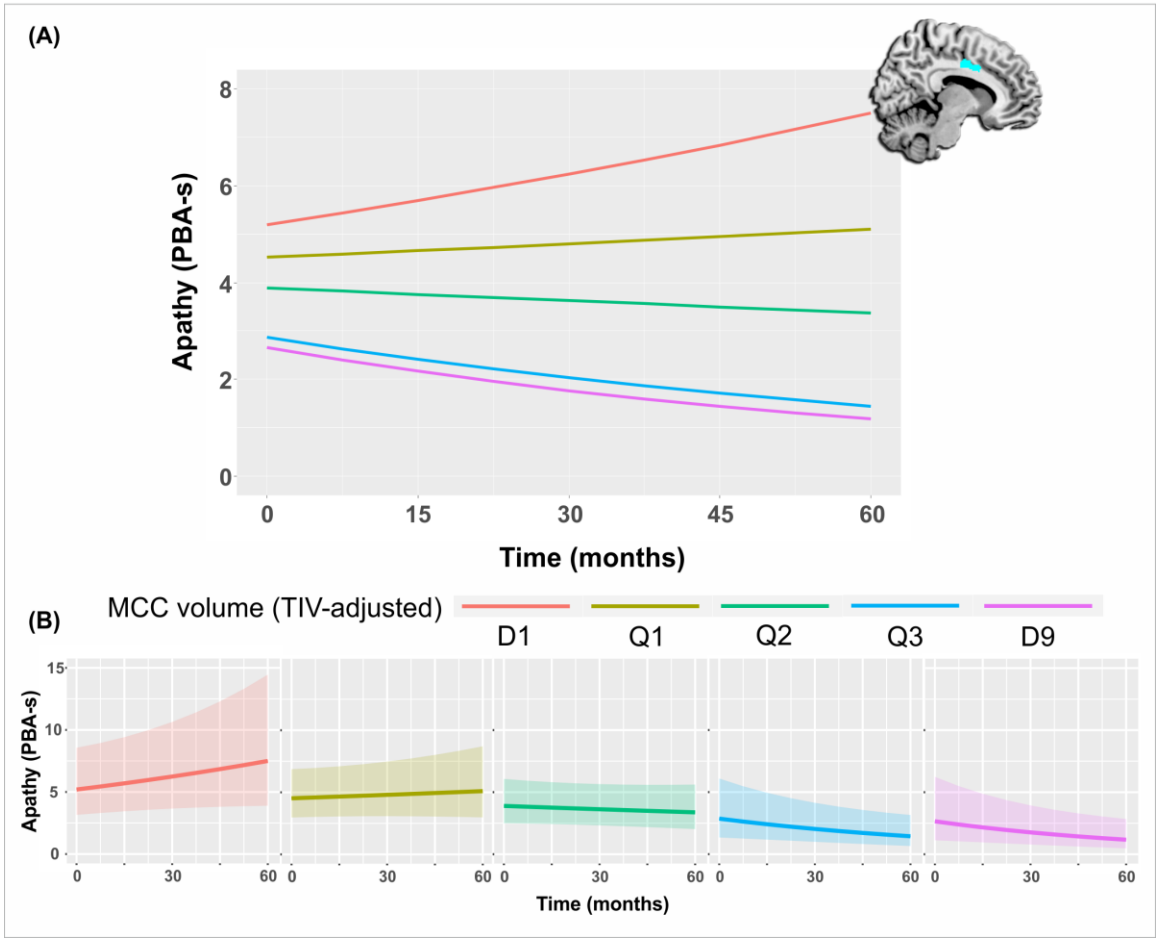

Figure 2. Smaller initial MCC volume predicts a faster rate of apathy development across time, demonstrated through Model 1.1 **(A)**, with split-view regression lines of model predictions at 95% confidence interval **(B)**. D1=first decile; D9=ninth decile; MCC=middle cingulate cortex; PBA-s=short-Problem-Behavior Assessment; Q1=first quartile; Q2=median; Q3=third quartile; TIV=total intracranial volume.

Table 1. Sociodemographic information at baseline.

Characteristics	Pre-HD	Manifest-HD	HD all
N	22	23	45
Sex (f/m)	18/4	13/10	31/14
Age (years)	38.32 ± 9.2	52.48 ± 10.1	45.56 ± 11.9
Education (years)	13.95 ± 2.9	10.74 ± 2.9	12.31 ± 3.3
CAP	82.89 ± 19.2	113.14 ± 19.2	98.35 ± 24.4
UHDRS-TMS	2.00 ± 3.7	22.57 ± 12.6	12.51 ± 13.9
UHDRS-cogscore	292.77 ± 62.4	183.14 ± 58.0, *N* = 21	239.23 ± 81.4, *N* = 43
TFC	12.79 ± 0.7, *N* = 19	11.26 ± 2.0	11.95 ± 1.7, *N* = 42
PBA-s total	12.50 ± 18.7	18.04 ± 17.6	15.33 ± 18.1
Apathy	2.55 ± 4.3	5.61 ± 5.0	4.11 ± 4.9
Perseveration	2.45 ± 4.4	2.96 ± 3.3	2.71 ± 3.8
Depressed mood	2.45 ± 3.5	1.70 ± 2.7	2.07 ± 3.1
Irritability	1.00 ± 2.2	2.70 ± 3.7	1.87 ± 3.2
Anxiety	1.41 ± 2.2	1.57 ± 2.8	1.49 ± 2.5
Paranoia	1.09 ± 3.5	0.57 ± 2.5	0.82 ± 3.0
Anger/aggression	0.41 ± 1.7	0.91 ± 2.0	0.67 ±1.8
Obsessive-compulsive	0.18 ± 0.9	1.04 ± 2.8	0.62 ± 2.1
Hallucinations	0.23 ± 0.9	0.52 ± 2.5	0.38 ± 1.9
Suicidal ideation	0.68 ± 1.8	0.09 ± 0.3	0.38 ± 1.3
Disorientation	0.05 ± 0.2	0.39 ± 0.9	0.22 ± 0.7

Data presented as *mean ± standard deviation*. *N* (number of participants) detailed in individual cells where differing. Premotor manifest and motor manifest participants grouped based on their Unified Huntington's Disease Rating Scale diagnostic confidence score for motor abnormalities at the first visit(23).
CAP=standardized age-CAG product(24); f=females; HD=Huntington's Disease; m=males; Manifest-HD=motor manifest; PBA-s=short-Problem Behavior Assessment; Pre-HD=premotor manifest; TFC=Total Functional Capacity; UHDRS-cogscore=Unified Huntington's Disease Rating Scale total cognitive score(23); UHDRS-TMS=Unified Huntington's Disease Rating Scale total motor score(23).

Table 2. Apathy and cognitive decline as predicted by right middle cingulate volume.

Models	*β* Estimate	*SE*	*Z* value	*P* value
Model 1.0 – PBA-s apathy null AIC = 738.1; *W* = 0.227				
CAP	0.199	0.115	1.724	n.s.
Neuropsychiatric disturbances[a]	0.223	0.063	3.573	< 0.001
Time[b]	-0.010	0.076	-0.130	n.s.
Model 1.1 – PBA-s apathy AIC = 735.7; *W* = 0.773				
Right MCC volume	-0.183	0.134	-1.363	n.s.
CAP	0.128	0.119	1.073	n.s.

Neuropsychiatric disturbances[a]	0.218	0.060	3.649	< 0.001
Time[b]	-0.047	0.068	-0.690	n.s.
Right MCC volume × Time	-0.184	0.075	-2.473	0.013
Model 2.0 – PBA-s depression null AIC = 835.4; *W* = 0.702				
CAP	-0.110	0.191	-0.574	n.s.
Neuropsychiatric disturbances[a]	0.623	0.087	7.116	<0.001
Time[b]	0.277	0.218	1.270	n.s.
Model 2.1 – PBA-s depression AIC = 837.1 ; *W* = 0.298				
Right MCC volume	-0.383	0.254	-1.506	n.s.
CAP	-0.221	0.215	-1.029	n.s.
Neuropsychiatric disturbances[a]	0.618	0.088	7.060	<0.001
Time[b]	0.306	0.220	1.392	n.s.
Right MCC volume × Time	-0.230	0.215	-1.071	n.s.
Model 3.0 – UHDRS-cogscore null AIC = 1778.2; *W* = 0.061				
CAP	-0.273	0.055	-4.950	<0.001
Neuropsychiatric disturbances[a]	-0.026	0.011	-2.321	0.020
Time[b]	-0.029	0.021	-1.393	n.s.
Model 3.1 – UHDRS-cogscore AIC = 1772.7; *W* = 0.939				
Right MCC volume	0.124	0.058	2.133	0.033
CAP	-0.225	0.059	-3.836	<0.001
Neuropsychiatric disturbances[a]	-0.025	0.011	-2.291	0.022
Time[b]	-0.046	0.020	-2.274	0.023

Right MCC volume × Time	0.046	0.018	2.521	0.012

All regression estimates are standardized. *P*-values significant at $P<0.05$.

[a] Neuropsychiatric disturbances evaluated through the PBA-s, calculated by subtracting the apathy sub-score from the total score in Model 1, the depression sub-score from the total score in Model 2, and utilizing the total PBA-s score (without subtractions) in Model 3.

[b] Time in days (accumulative, time at first assessment is zero).

AIC=Akaike's information criteria; CAP=standardized age-CAG product(1); MCC=middle cingulate cortex; *SE*=standard error; PBA-s=short-Problem Behavior Assessment(2); UHDRS-cogscore=Unified Huntington's Disease Rating Scale total cognitive score(3); *W*=Akaike's information criteria weight(4,5).

Supplemental information

1. Sociodemographic and clinical data

Table S1. Sociodemographic information for longitudinal voxel-based morphometry cohort (at baseline).

Characteristics	Pre-HD	Manifest-HD	HD all
N	15	18	33
Sex (f/m)	14/1	9/9	23/10
Age (years)	41.13 ± 9.4	50.78 ± 10.	46.39 ± 10.8
Education (years)	14.07 ± 2.8	10.83 ± 2.8	12.30 ± 3.2
CAP	86.27 ± 22	109.87 ± 17, *N* = 16	99.14 ± 22.6
UHDRS-TMS	2.07 ± 3.8	18.44 ± 8.2	11.00 ± 10.5
UHDRS-cogscore	256.33 ± 54	164.50 ± 41, *N* = 16	208.94 ± 66, *N* = 31
TFC	12.92 ± 0.29, *N* = 12	11.50 ± 1.5	12.07 ± 1.4
PBA-s total	10.47 ± 18	12.56 ± 12	11.61 ± 15
Apathy	2.40 ± 4.4	4.17 ± 4.4	3.36 ± 4.4
Perseveration	2.40 ± 4.5	2.22 ± 2.8	2.30 ± 3.6
Depressed mood	2.20 ± 3.4	1.06 ± 1.8	1.58 ± 2.7
Irritability	0.93 ± 2.3	2.56 ± 3.9	1.82 ± 3.3
Anxiety	1.00 ± 2.1	0.78 ± 1.3	0.88 ± 1.7
Paranoia	0.27 ± 1.0	0.06 ± 0.24	0.15 ± 0.71
Anger/aggression	0.53 ± 2.1	0.39 ± 1.4	0.46 ± 1.7
Obsessive-compulsive	0.27 ± 1.0	1.00 ± 2.9	0.67 ± 2.3
Hallucinations	0.07 ± 0.26	0.00 ± 0.00	0.03 ± 0.17
Suicidal ideation	0.40 ± 1.5	0.11 ± 0.32	0.24 ± 1.1
Disorientation	0.00 ± 0.00	0.22 ± 0.55	0.12 ± 0.42

Data presented as *mean* ± *standard deviation*. *N* (number of participants) detailed in individual cells where differing. Premotor manifest and motor manifest participants grouped based on their Unified Huntington's Disease Rating Scale diagnostic confidence score for motor abnormalities at the first visit(1).

CAP=standardized age-CAG product(2); f=females; HD=Huntington's Disease; m=males; Manifest-HD=motor manifest; PBA-s=Problem Behavior Assessment, short-form(3); Pre-HD=premotor manifest; TFC=Total Functional Capacity; UHDRS-TMS=Unified Huntington's Disease Rating Scale total motor score(1); UHDRS-cogscore=Unified Huntington's Disease Rating Scale total cognitive score(1).

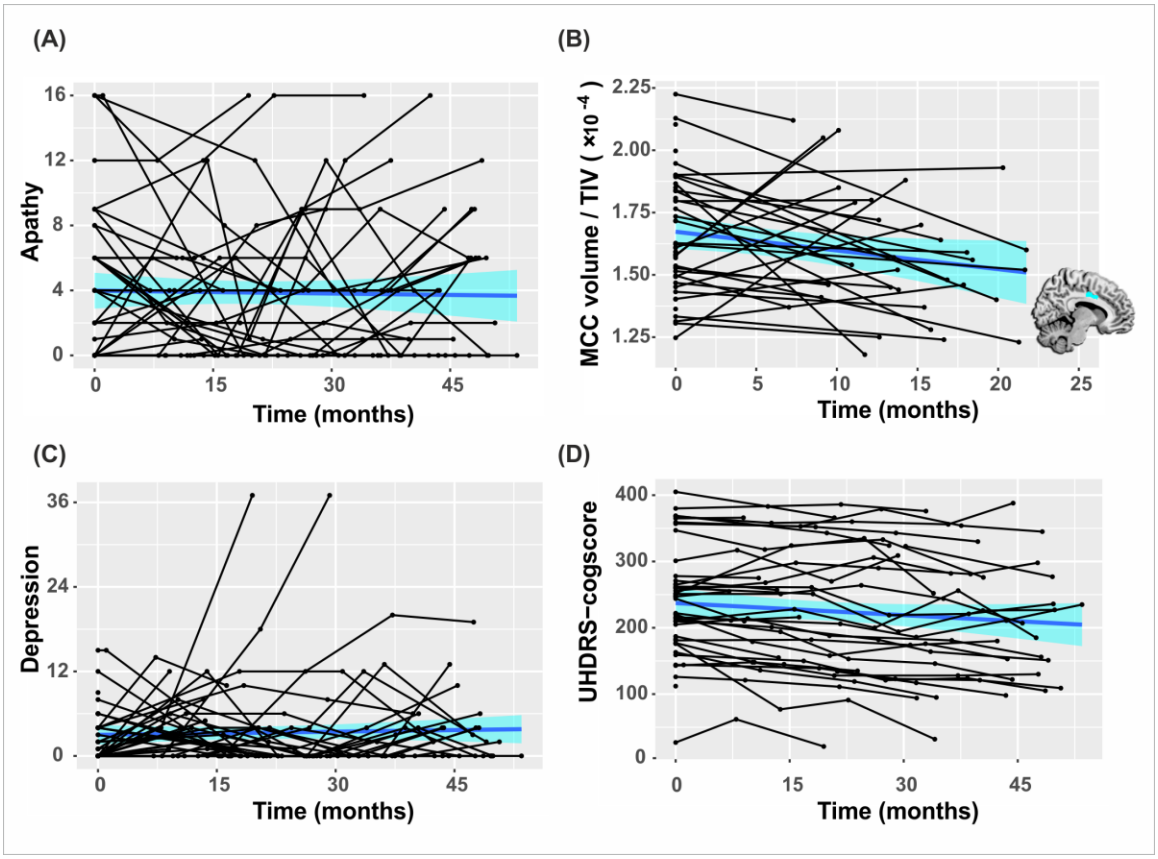

Figure S1. Raw longitudinal data for each participant, illustrating apathy (A), TIV-adjusted MCC volume (B), depression (C), and cognition (D). Fitted linear regression models with respective 95% confidence intervals presented in blue. Mask of MCC volume inlaid. MCC=middle cingulate cortex; TIV=total intracranial volume.

2. Longitudinal voxel-based morphometry (VBM)

Table S2. Longitudinal VBM of GMV and PBA-s apathy in premanifest HD individuals.

Anatomical region	Cluster size	T value	*P* value	MNI Coordinates (*x,y,z*)
Premanifest HD				
L Cuneus	879	5.31	< 0.001	-5 -95 18
R Inferior occipital lobe	948	5.09	< 0.001	38 -87 5
R MCC	320	4.89	< 0.001	8 5 30

P values were significant at $P<0.005$ (uncorrected) and a threshold of $P<0.05$ applied at cluster level, with a minimum cluster size of 100 contiguous voxels.

BA=Brodmann area; CAP=standardized age-CAG product(2); dlPFC=dorsolateral prefrontal area; GMV=gray matter volume; MCC=middle cingulate cortex; MNI=Montreal Neurological Institute; PBA-s=short-Problem Behavior Assessment(3); VBM=voxel-based morphometry.

3. Generalized linear mixed-effects models

3.1. Analysis Code in R

```
library(xlsx)
library(glmmTMB)
library(qpcR)
library(performance)

setwd('~/Downloads')
df <- read.xlsx('Mixed_models_data_131020_all.xlsx', sheetIndex=3)

df$ID <- as.integer(1:nrow(df))

lf <- reshape(df, idvar='Code', varying=7:(ncol(df)-1), sep="_",
direction='long')
lf <- lf[,c('ID','days','CAP','PBArest','Apathy','nACC_1')]
lf <- lf[order(lf$ID),]

lf$days <- as.numeric(scale(lf$days))
lf$CAP <- as.numeric(scale(lf$CAP))
lf$PBArest <- as.numeric(scale(lf$PBArest))
lf$nACC_1 <- as.numeric(scale(lf$nACC_1))

fit0 <- glmmTMB(Apathy ~ days + CAP + PBArest + (1+days||ID), zi=~1,
family=poisson, data=lf,control=glmmTMBControl(optCtrl=list(iter.max=1e3,
eval.max=1e3), profile=T))

fit1 <- glmmTMB(Apathy ~ nACC_1 * days + CAP + PBArest + (1+days||ID), zi=~1,
family=poisson, data=lf, control=glmmTMBControl(optCtrl=list(iter.max=1e3,
eval.max=1e3), profile=T))

results0 <- summary(fit0)
results1 <- summary(fit1)

anova(fit0,fit1)

x <- c(results0$AICtab[[1]], results1$AICtab[[1]])
akaike.weights(x)

check_collinearity(fit0, component = "conditional")
check_collinearity(fit1, component = "conditional")
```

Table S3. Apathy as predicted by cognitive decline

Models	***β* Estimate**	***SE***	***Z* value**	***P* value**
PBA-s apathy AIC = 830.1; *W* < 0.001				
PBA-s depression	-0.021	0.049	-0.435	n.s.
PBA-s apathy AIC = 665.8; *W* > 0.999				
UHDRS-cogscore	-0.284	0.100	-2.844	0.004

All regression estimates are standardized. *P*-values significant at *P*<0.05.
AIC=Akaike's information criteria; *SE*=standard error; PBA-s=short-Problem Behavior Assessment(3); UHDRS-cogscore=Unified Huntington's Disease Rating Scale total cognitive score(9); *W*=Akaike's information criteria weight(10,11).

4. Cross-sectional VBM

4.1. Cross-sectional VBM methods

We carried out cross-sectional morphometric analysis using the cat12 toolbox (http://www.neuro.uni-jena.de/cat/) in the SPM12 software package (Welcome Department of Imaging Neuroscience Group, London, UK) running on MATLAB (v17.a, Mathworks, Natick, MA) for all participants (*N*=45).

Specifically, unified segmentation(4) was applied to the structural T1-weighted images of each subject to estimate tissue gray matter probability maps, which were then normalized to a standard stereotactic space using the corresponding DARTEL transformations(5) to achieve spatial normalization in MNI space(6). The resulting gray matter normalized images were modulated by their Jacobian determinants and spatially smoothed using an 8mm FWHM surface-based smoothing kernel. Finally, images were visually inspected.

The total intracranial volume (TIV) was calculated as the sum of gray matter, white matter, and cerebrospinal fluid, averaged across both sessions.

The smoothed gray matter volume (GMV) images were entered into a voxel-wise multiple regression in order to examine the effect of GMV on apathy. TIV, age, education, sex, CAG-Age Product (CAP) scores(2), and non-apathetic neuropsychiatric disturbances, as measured by the short-Problem Behvaior Assessment (PBA-s), were entered into the model as covariates of no interest. The non-apathetic neuropsychiatric component was the sum of all ten additional (non-apathetic) neuropsychiatric factors evaluated with the PBA-s, allowing the examination of apathy as an independent neuropsychiatric symptom from the others. An explicit absolute masking with a threshold of 0.2 was applied in model selection (i.e., exclusively including voxels with>20% probability of being gray matter) to more selectively distinguish GM boundaries(7,8). For illustrative purposes, significant results were identified at three discrete significance levels (uncorrected) applied at voxel-level, with a minimum cluster size of 100 contiguous voxels: $P<.05$, $P<.01$, $P<.005$.

4.2. Cross-sectional VBM results

Utilizing a whole-brain approach, we found that higher apathy severity was significantly associated with reduced GMV across sub-cortical and cortical territories. Furthermore, the pattern of GMV was found to be similar both with and without controlling for the effects of CAP, a proxy measure of disease state, and non-apathetic neuropsychiatric symptoms. Results are presented when controlling for all aforementioned covariates of no-interest (Figure S2; Table S4).

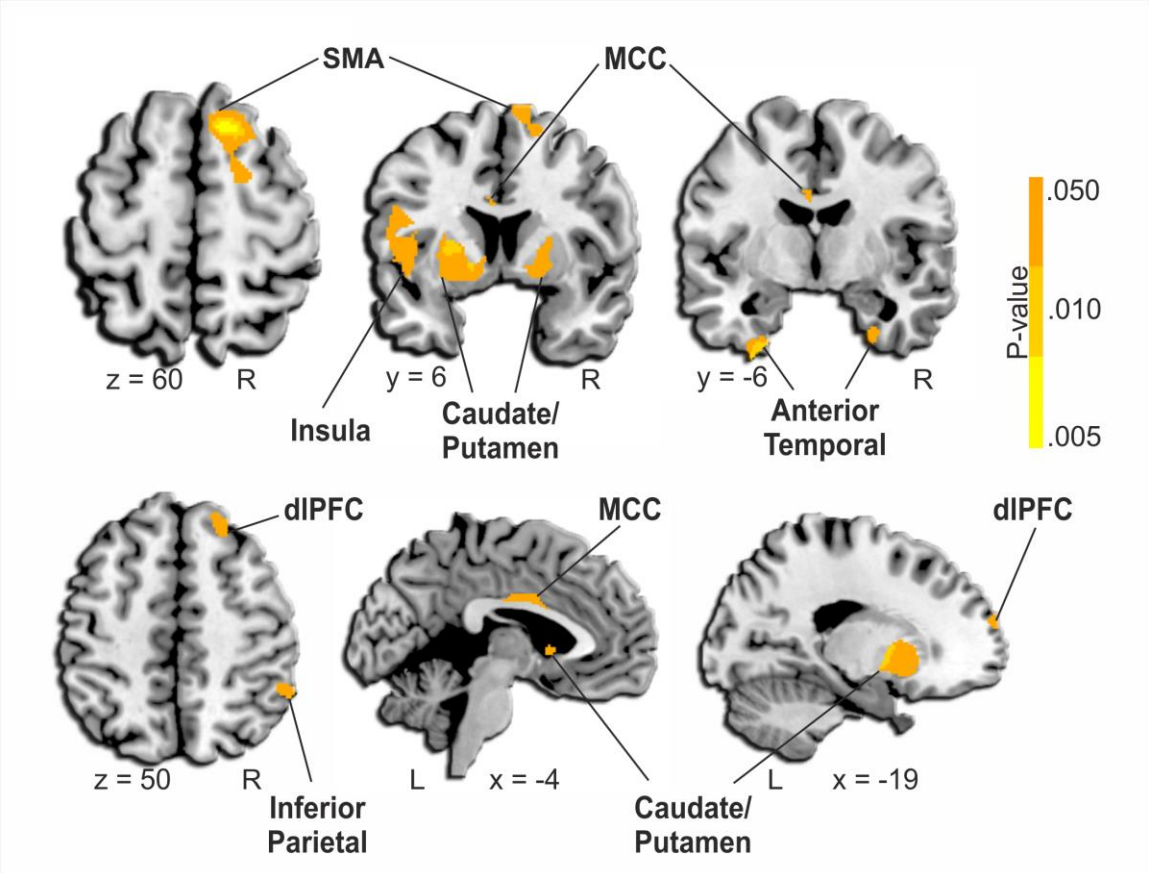

Figure S2. Results of cross-sectional voxel-based morphometry analysis with structural T1-weighted images. Slices display regions were lower gray matter volume is associated with higher apathy levels. For illustrative purposes, results are shown at three discrete significance levels (uncorrected) applied at voxel-level, with a minimum cluster size of 100 contiguous voxels: $P<.05$, $P<.01$, $P<.005$. Slice position is labeled in Montreal Neurological Institute coordinates. dlPFC=dorsolateral prefrontal area; L=left; MCC=middle cingulate cortex; R=right; SMA=supplementary motor area.

Table S4. Cross-sectional VBM analysis of GMV and PBA-s apathy.

Anatomical region	Cluster size	T value	*P* value	MNI Coordinates (*x*, *y*, *z*)
R SMA	1239	4.04	< 0.001	15 23 65
L Inferior temporal lobe	346	3.17	0.002	-29 -9 -45
L Pallidum/putamen/caudate head	1958	2.94	0.003	-20 2 2
L Insula (BA13)	965	2.85	0.004	-45 5 11
R Pallidum/putamen/caudate head	696	2.78	0.004	20 2 -3
L dlPFC (BA10)	107	2.50	0.008	-21 63 23
R Inferior parietal	121	2.45	0.010	57 -48 50
R Inferior temporal lobe	215	2.42	0.013	24 -15 -38
R dlPFC (BA10)	112	2.15	0.019	38 35 23
L MCC (BA24)	122	2.04	0.024	-6 -2 32

P values were significant at a threshold of $P<0.05$ applied at voxel-level, with a minimum cluster size of 100 contiguous voxels.
BA=Brodmann area; CAP=standardized age-CAG product(2); dlPFC=dorsolateral prefrontal area; GMV=gray matter volume; MCC=middle cingulate cortex; MNI=Montreal Neurological Institute; PBA-s=short-Problem Behavior Assessment(3); SMA=supplementary motor area; VBM=voxel-based morphometry.

References

1. Huntington Study Group. Unified Huntington's disease rating scale: Reliability and consistency. Movement Disorders. 1996 Mar 1;11(2):136–42.

2. Ross CA, Aylward EH, Wild EJ, Langbehn DR, Long JD, Warner JH, et al. Huntington disease: natural history, biomarkers and prospects for therapeutics. Nature Reviews Neurology. 2014 Apr;10(4):204–16.

3. Callaghan J, Stopford C, Arran N, Boisse M-F, Coleman A, Santos RD, et al. Reliability and Factor Structure of the Short Problem Behaviors Assessment for Huntington's Disease (PBA-s) in the TRACK-HD and REGISTRY studies. The Journal of Neuropsychiatry and Clinical Neurosciences. 2015 Jan;27(1):59–64.

4. Ashburner J, Friston KJ. Unified segmentation. Neuroimage. 2005 Jul 1;26(3):839–51.

5. Ashburner J. A fast diffeomorphic image registration algorithm. Neuroimage. 2007 Oct 15;38(1):95–113.

6. Ashburner J, Friston KJ. Computing average shaped tissue probability templates. Neuroimage. 2009 Apr 1;45(2):333–41.

7. James CE, Oechslin MS, Van De Ville D, Hauert C-A, Descloux C, Lazeyras F. Musical training intensity yields opposite effects on grey matter density in cognitive versus sensorimotor networks. Brain Struct Funct. 2014 Jan;219(1):353–66.

8. Ashburner J. VBM Tutorial [Internet]. 2010. Available from: http://www.fil.ion.ucl.ac.uk/~john/misc/ VBMclass10.pdf

9. Huntington Study Group. Unified Huntington's disease rating scale: Reliability and consistency. Movement Disorders. 1996 Mar 1;11(2):136–42.

10. Burnham K, Anderson D. Model Selection and Multimodal Inference. New York: Springer; 2002.

11. Long J. Data Analysis for Behavioral Sciences Using R. Thousand Oaks, CA: Sage Publications Inc.; 2011.